International Journal of General Medicine

Dovepress
Taylor & Francis Group

Open Access Full Text Article

ORIGINAL RESEARCH

Potential Diagnostic Value of Circular RNA hsa_circ_0008882 in Rheumatic Valvular Heart Disease

YunSong Hu[1,2,*], Ni Li[1,*], LeBo Sun[1], HuoShun Shi[1], GuoFeng Shao[1], LinWen Zhu[1]

[1]Department of Cardiothoracic Surgery, The Affiliated Lihuili Hospital of Ningbo University, Ningbo, Zhejiang, 315000, People's Republic of China; [2]Health Science Center, Ningbo University, Ningbo, Zhejiang, 315211, People's Republic of China

*These authors contributed equally to this work

Correspondence: GuoFeng Shao; LinWen Zhu, Department of Cardiothoracic Surgery, The Affiliated Lihuili Hospital of Ningbo University, No. 57 Xingning Road, Yinzhou District, Ningbo, Zhejiang, 315000, People's Republic of China, Email sgf1958@sina.com; lhlzhulinwen@nbu.edu.cn

Aim: To investigate the involvement of circular RNA (circRNA) in the pathogenesis of rheumatic valvular heart disease (RVHD) and its potential use as a diagnostic biomarker.

Methods: Three differentially expressed circRNAs in RVHD were selected. Four pairs of RVHD valve tissues and non-RVHD valve tissues were verified. Plasma samples from 41 RVHD patients and 39 healthy controls were analyzed to investigate the relationship between hsa_circ_0008882 expression levels and clinical-pathological characteristics in RVHD patients, evaluating its diagnostic value for RVHD. Additional plasma samples from 47 RVHD patients and 30 controls, along with 38 valve tissues, were collected to validate the expression of downstream target genes CAMTA2 and APLN. LASSO regression combined with multivariate logistic regression analysis was employed to identify independent risk factors. The interaction between hsa_circ_0008882 and hsa-miR-4739 was validated through dual luciferase reporter assays.

Results: The expression of hsa_circ_0008882 was significantly upregulated in both plasma and valve tissue samples from RVHD patients. Plasma hsa_circ_0008882 demonstrated moderate discriminatory ability for RVHD, with an AUC of 0.707 (95% CI: 0.591–0.823), a sensitivity of 58.5%, and a specificity of 82.1% at the optimal cutoff value. Its expression level showed significant positive correlations with multivalvular heart disease, left atrial diameter, and pulmonary artery systolic pressure. After LASSO regression screening, multivariate analysis confirmed hsa_circ_0008882 as an independent risk factor for RVHD (OR = 3.73, 95% CI: 1.75–7.95). Mechanistic exploration revealed that hsa_circ_0008882 directly binds to hsa-miR-4739, and its potential target genes CAMTA2 and APLN were both upregulated in plasma and tissue samples from RVHD patients.

Conclusion: Hsa_circ_0008882 plays an essential role in RVHD, and its plasma expression levels may serve as a potential auxiliary diagnostic indicator for RVHD.

Keywords: circular RNA, hsa_circ_0008882, rheumatic valvular heart disease, diagnosis, noncoding RNA

Introduction

Rheumatic heart disease (RHD) is a consequence of rheumatic fever, which arises from a throat infection by Group A Streptococcus (*Streptococcus pyogenes*). Acute rheumatic fever (ARF) is most common among children aged 5 to 15. Yet, the likelihood of experiencing a first episode of rheumatic fever consistently falls after adolescence, and the incidence generally wanes as individuals age.[1] Approximately 40 million people worldwide were affected by RHD in 2019, with 2.8 million new cases occurring every year. The global mortality rate is nearly 300,000, with the median age being 28.7 years.[2,3] Hospital records on RHD focus on moderate-to-severe cases, implying that the real prevalence, largely consisting of mild cases, might be considerably greater. RHD faces significant risk due to the lack of antibiotics, overcrowded areas, and poor sanitation. In both developing and developed countries, specific marginalized communities face a high rate of RHD.[4]

Received: 19 August 2025
Accepted: 27 October 2025
Published: 14 November 2025

Globally, RHD is the leading cause of valve disease, primarily impacting the mitral and aortic valves, and often presenting as regurgitation in children and young adults who are especially susceptible to strep pharyngitis. Rheumatic valvular heart disease (RVHD) is a key factor driving the demand for heart surgeries in China, as it causes atrial fibrillation, heart failure, and pulmonary hypertension.[5] In RVHD, the left heart is typically affected, primarily targeting the mitral valve, with the aortic and tricuspid valves also involved.[6] Cardiovascular abnormalities such as ruptured aortic dissection may remain undetected clinically until sudden cardiac death occurs, underscoring the importance of biomarkers for the early diagnosis of cardiovascular disease.[7]

Transthoracic echocardiography (TTE) is the main diagnostic tool for RVHD. Echocardiography in clinical scenarios may detect ambiguous valvular lesions, and the World Heart Federation criteria can frequently assist in distinguishing RVHD from normal and diagnosing subclinical carditis related to ARF.[5] Indicators for diagnosing RVHD include erythrocyte sedimentation rate, C-reactive protein, mucin, protein electrophoresis, circulating immune complex, serum total complement, complement C3, IgG, IgM, IgA, B lymphocyte detection, and anti-myocardial antibody. These tests lack strong sensitivity and specificity, especially during the chronic phase, highlighting the need for biomarkers to aid in RVHD diagnosis and treatment.

Circular RNA (circRNA) was first described in 1976.[8] These are endogenous closed-loop single-stranded RNAs in eukaryotes with cell- and tissue-specific expression patterns.[9] CircRNA, characterized by its stable circular structure, provides greater exonuclidene inhibition than linear RNA and can be found in exosomes and plasma. The roles of circRNA involve (i) controlling transcription, (ii) providing binding sites for microRNA (miRNA) that function as endogenous RNA or miRNA sponges, thereby inhibiting miRNA activity and indirectly influencing the expression of miRNA target genes at the post-transcriptional level, (iii) translating protein, and (iv) interacting with RNA binding protein. In addition, some circRNAs may affect alternative splicing.[10] Due to their high stability, expression, and specificity, circRNA is emerging as a promising biomarker for many human diseases.

CircRNA has been extensively researched in cardiovascular conditions like coronary heart disease, hypertension, atherosclerosis, and cardiomyopathy, but there is limited research on RVHD. Therefore, exploring its role in RVHD is significant for disease research.[11,12] Early analysis of circRNA in samples from human heart tissue demonstrated that certain circRNA were found in high abundance.[13] Abnormal circRNA expression can indicate the development and progression of heart disease. Hence, heart disease prediction is feasible through circRNA expression measurement, but collecting and analyzing heart tissue samples from patients poses clinical difficulties. For circRNA expression levels to be effective biomarkers for heart disease, they need to be evaluated in samples that are easy to collect, such as blood, to predict the progression of heart disease. Because blood comprises various substances from multiple organs, its use as a heart disease indicator necessitates that the transcript levels in heart tissue cells correspond to the levels detected in the blood. Research has explored this significant issue by examining the transcriptome in the heart and blood.[14,15]

This study utilized a circRNA microarray to investigate circRNA expression in the plasma of three RVHD patients and three controls. CircRNAs were deemed differentially expressed if they exhibited a fold-change exceeding 2 and a P-value below 0.05. The target circRNA hsa_circ_0008882 was identified through screening using circBase and GEO databases. It exhibited a significant and stable upward trend in chip analysis, and its host genes possess potential functions in the cardiovascular system, making it the target for subsequent research. Its expression levels were validated in an expanded sample size and its potential as a biomarker for RVHD was explored.

Materials and Methods

Clinical Specimens

This study recruited participants in two consecutive phases.

Phase 1 (Core Discovery Cohort): Between January and June 2023, 41 patients with RVHD and 39 healthy controls were enrolled, and their plasma samples were collected. Concurrently, this phase collected 4 RVHD valve tissues (RVHD tissues were explicitly sourced from patients undergoing mitral valve replacement due to severe rheumatic mitral valve disease) and 4 non-RVHD valve tissues (primarily from patients with non-rheumatic, non-infectious valvular diseases, such as mitral valve mucoid degeneration and bicuspid aortic valve). This cohort was used for validation of hsa_circ_0008882, assessment of its diagnostic value, and analysis of its relationship with clinical parameters.

Phase 2 (Independent Validation Cohort): Between July and December 2023, to further advance genetic and mechanistic exploration studies, an additional 47 RVHD patients were recruited and their plasma samples collected. Concurrently, 11 RVHD valve tissues and 27 non-RVHD valve tissues were obtained. Plasma samples from 30 healthy controls were also sourced from participants screened under identical criteria during this phase. This cohort was specifically designated to validate the expression of potential target genes (CAMTA2 and APLN).

Inclusion criteria for RVHD patients included physical examination, electrocardiogram (ECG), chest radiography, and TTE. Normal levels of erythrocyte sedimentation and anti-hemolysin O indicated no rheumatic activity. Patients with recent acute heart failure, myocardial infarction, or other complications were also excluded. A control group was formed with thirty-nine healthy individuals who had normal physical exams, and TTE was part of the screening, leading to the collection of 30 cases. The Ethics Committee of Ningbo Medical Center Lihuili Hospital approved all research protocols (IRB No.KY2022PJ222) and written informed consent was provided by all patients prior to the study start. Figure 1 shows the detailed sample workflow.

Collection and Storage of Plasma and Tissue Samples

Three milliliters of peripheral venous blood were placed into an anticoagulant tube containing EDTA, centrifuged at 3000 rpm for 15 min, and the upper light yellow plasma layer was removed in a 2-mL RNase-free Eppendorf tube, and stored at –80 °C until use. The tissue samples were stored at –80 °C.

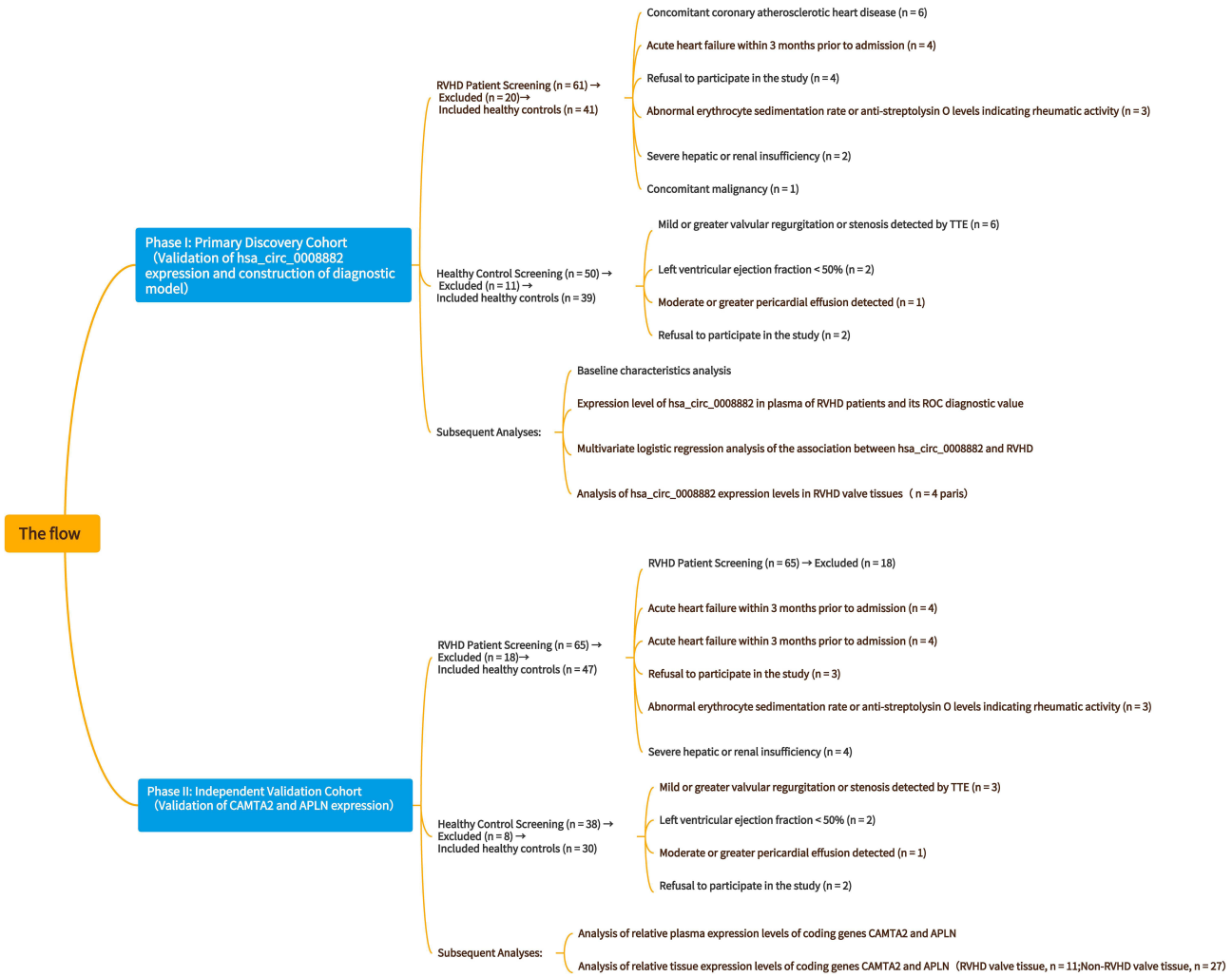

Figure 1 Study sample inclusion and analysis process.

https://doi.org/10.2147/IJGM.S558257

circRNA Microarray Assays

All blood samples were collected as 3 mL peripheral venous blood using vacuum blood collection tubes on the morning before surgery, following the participant's admission to the hospital. The blood was immediately transferred into anticoagulant tubes containing ethylenediaminetetraacetic acid. Within 2 hours of collection at 4°C, the samples were centrifuged at 3000 rpm for 15 min, the pale yellow supernatant was carefully aspirated, and aliquoted into 2 mL RNase-free centrifuge tubes (Eppendorf tubes). Tissue samples obtained during heart valve replacement surgery were rinsed with sterile saline and promptly aliquoted. All plasma and tissue aliquots were immediately transferred to a −80°C ultra-low temperature freezer for long-term storage until RNA extraction. To ensure biomolecular quality, each aliquot used in this study underwent only one freeze-thaw cycle.

Total RNA Extraction and Reverse Transcription

Total RNA in plasma and tissue was extracted using TRIzol LS reagent (Invitrogen) according to the manufacturer's instructions. The circRNA expression profile data used in this study are deposited in the GEO database under accession number GSE168932.

Total RNA was quantified using the NanoDrop ND-1000. Subsequently, total RNA was digested with RNase R (Epicentre, Inc.) to remove linear RNA and enrich circular RNA. The enriched circular RNA was amplified and transcribed into fluorescent cRNA using the Arraystar Super RNA Labeling Kit. The labeled cRNA was hybridized with the Arraystar Human circRNA Array V2 (8x15K, Arraystar). Following hybridization, the array was scanned using the Agilent Scanner G2505C.

Image data were analyzed using Agilent Feature Extraction software (version 11.0.1.1), followed by quantile normalization and subsequent data processing via the limma package in R software. Differentially expressed circRNAs were identified based on the criteria: fold change (FC) > 2 and P-value < 0.05.[16]

RT-qPCR

The Mx3005P RT-qPCR system (Stratagene) was utilized to amplify hsa_circ_0008882 using NovoStart® SYBR qPCR SuperMix Plus (Novoprotein, China). The specific convergence primer sequence of hsa_circ_0008882 is shown in Table 1. To ensure specific detection of circular RNA, divergent primers were designed targeting the reverse splice junction of hsa_circ_0008882. Melt curve analysis was performed to exclude non-specific amplification and primer dimer interference. Glyceraldehyde 3-phosphate dehydrogenase (GAPDH) and ACTIN were used as external references, and protein-coding genes CAMTA2 and APLN were used as subsequent detection genes, and their priming sequences were shown in Table 1. The primer was synthesized by Tsingke (China). Data were analyzed by the $2^{-\Delta CT}$ method.

Dual Luciferase Reporter Assay

The wild-type and mutant plasmids were transfected into 96-well plates with lysis by passive lysis buffer (100 μL/well) 48 h later. After adding Luciferase Assay Reagent II (LAR II) (100 μL/well), firefly luciferase activity was detected as the luminescence value of the reporter gene, and then Stop&Glo Reagent (100 μL/well) was used to measure the renilla

Table 1 Primer Sequence of hsa_circ_0008882, GAPDH, GAPDH, ACTIN, CAMTA2 and APLN

Target ID	Primer Sequence, 5′-3′
hsa_circ_0008882	F:GCAGCCTAGCATTAGCAGGAA
	R:GAGGGAGGTTGAAGTGAGAGGT
GAPDH	F:AAGGTGAAGGTCGGAGTCAA
	R:AATGAAGGGGTCATTGATGG
ACTIN	F:ACAGGCATCGTGATGGATTCT
	R:CAGCAGTGGTGGTGAAGTTAT
CAMTA2	F:TTGCACAGACTGGGGCTATG
	R:GTCCCTCTTCCCGGTTCG
APLN	F:ACTGGCCCCAAGTATCAAGC
	R:TACAGGCGTGACAACCCAAA

luciferase activity, the internal reference gene luminescence value. The values of firefly fluorescence detection and renilla fluorescence were normalized, and the calculated value of the normalized reaction was the ratio of the two.

Statistical Analysis

Statistical analyses were performed using SPSS Statistics 20.0 (IBM, USA) and the R language. Continuous variables were first assessed for normality using the Shapiro–Wilk test. Data meeting normality requirements were expressed as mean ± standard deviation, with intergroup comparisons performed using two-tailed Student's t-tests. Data failing normality were presented as median (interquartile range), with intergroup comparisons conducted using the Mann–Whitney *U*-test. Categorical variables were reported as case counts (percentages), with intergroup comparisons performed using chi-square tests. Spearman correlation analysis was employed to investigate the relationship between hsa_circ_0008882 expression levels and clinical parameters, with results adjusted using the Benjamini-Hochberg method. To construct a robust diagnostic model and prevent overfitting, the following strategy was adopted. First, continuous variables (age, BMI, hsa_circ_0008882) were Z-score standardized. Subsequently, the LASSO regression model was employed to select the optimal penalty coefficient (λ) through 10-fold cross-validation, thereby identifying the most relevant predictors for RVHD from all clinical covariates. Finally, the variables selected by LASSO were incorporated into a multivariate logistic regression model to calculate their odds ratios (OR) and 95% confidence intervals (CI). The diagnostic discriminatory ability of hsa_circ_0008882 was evaluated using the receiver operating characteristic curve (ROC curve) and area under the curve (AUC). The optimal cutoff value was determined by maximizing the Youden index, and corresponding metrics including sensitivity, specificity, positive/negative likelihood ratios were reported. All statistical analyses employed two-sided tests, with $P < 0.05$ indicating statistically significant differences.

Results

circRNA Chip Screening for RVHD-Associated Differentially Expressed circRNAs and the Specificity of hsa_circ_0008882

To screen circRNAs associated with RVHD, circRNA microarray analysis was performed on plasma samples from 3 RVHD patients and 3 healthy controls. Volcano plots visually displayed the differential expression patterns of all circRNAs (Figure 2A). Concurrently, hierarchical clustering analysis revealed that differentially expressed circRNAs clearly distinguished RVHD samples from control samples (Figure 2B). Based on the criteria of fold change (FC) > 2 and raw p-value < 0.05, multiple differentially expressed circRNAs were identified. After multiple testing correction using the Benjamini-Hochberg method, the adjusted P-value (FDR) for the finally selected hsa_circ_0008882 remained below 0.05, indicating statistically significant differential expression. Combining searches in the circBase and GEO databases, hsa_circ_0008882 was selected as the focus for subsequent studies due to its potential functional role in the cardiovascular system and its most significant differential expression in the microarray. Specific convergent primers were designed for hsa_circ_0008882. Melt curve analysis validated the RT-qPCR primers (Figure 2C). The amplification product exhibited a single peak on the melt curve, indicating no non-specific amplification or primer dimer formation.

hsa_circ_0008882 Expression in Valve Tissues of RVHD Patients

hsa_circ_0008882 expression was measured in four RVHD and non-RVHD valve tissue pairs (Figure 3). hsa_circ_0008882 levels were significantly higher in RVHD valve tissue than in non-RVHD valve tissue.

hsa_circ_0008882 Expression in Plasma of RVHD Patients

hsa_circ_0008882 expression levels were measured in plasma samples from 41 RVHD patients and 39 controls (Figure 4A). Microarray analysis confirmed that hsa_circ_0008882 levels were significantly greater in RVHD patients than in the control group.

Figure 4B illustrates the use of ROC curve analysis to determine the diagnostic role of hsa_circ_0008882 in RVHD. The RVHD group had an AUC of 0.707 (95% CI: 0.591–0.823, $p < 0.01$), indicating moderate diagnostic performance.

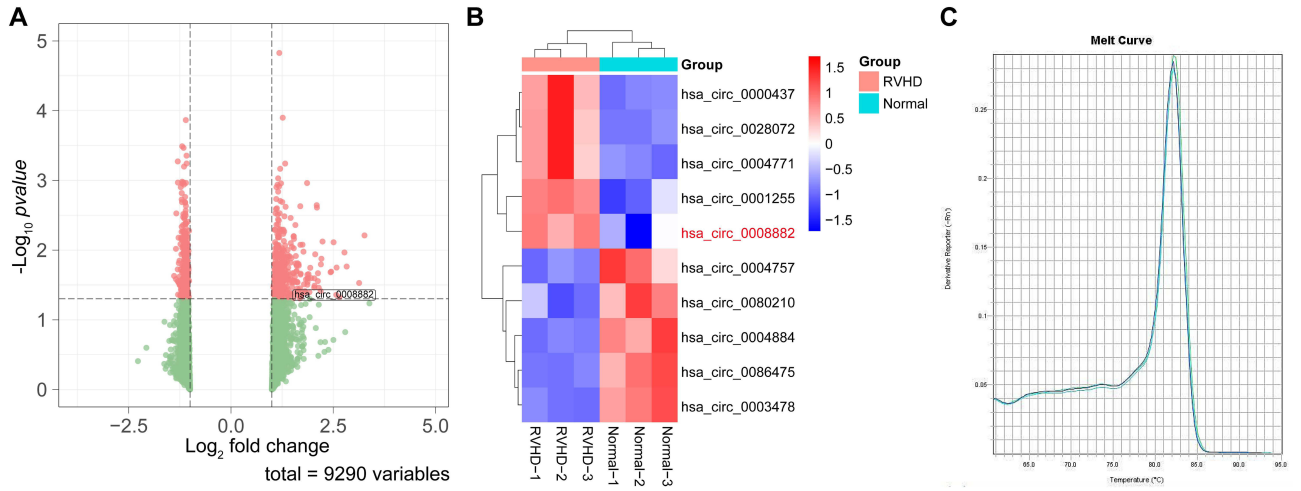

Figure 2 circRNA chip screening for RVHD-associated differentially expressed circRNAs and specificity analysis of hsa_circ_0008882. (**A**) Volcano plot of differentially expressed circRNAs. Gray dots indicate circRNAs without significant differences. Red dots represent significantly upregulated circRNAs (Fold Change > 2, FDR-adjusted *P*-value < 0.05). Green dots denote significantly downregulated circRNAs (Fold Change < 0.5, FDR-adjusted *P*-value < 0.05). (**B**) Hierarchical clustering heatmap of significantly differentially expressed circRNAs. Expression patterns between the RVHD group (representative samples n=3) and the control group (representative samples n=3). Red indicates high expression, blue indicates low expression. (**C**) hsa_circ_0008882 RT-qPCR product melting curve analysis.

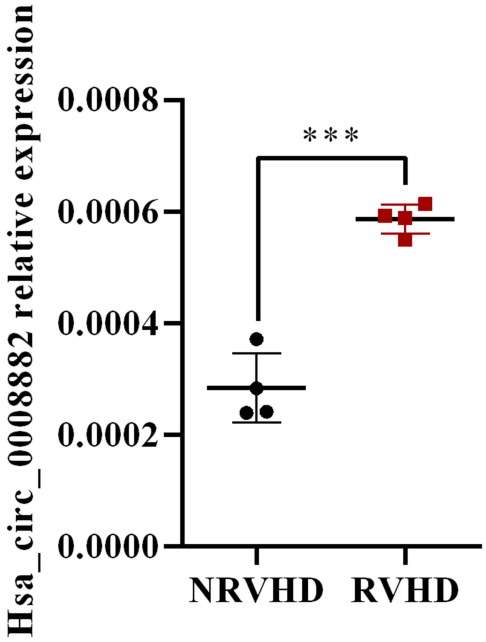

Figure 3 Expression level of hsa_circ_0008882 in RVHD valve tissue. ***p < 0.001.

The optimal cutoff value determined by maximizing the Youden index was 0.507, yielding a sensitivity of 58.5% and specificity of 82.1%. Additionally, the positive predictive value was 77.4%, and the negative predictive value was 65.3%.

hsa_circ_0008882 Expression and Its Relationship with Multivalvular Heart Disease and Echocardiography

To investigate the clinical significance of hsa_circ_0008882, its expression levels were analyzed for correlations with key clinical parameters. As shown in Table 2, hsa_circ_0008882 expression levels exhibited significant positive correlations with multivalvular heart disease (Pearson r = 0.286, $p = 0.010$; Spearman ρ = 0.361, $p = 0.001$). Furthermore, its expression level was closely associated with echocardiographic parameters reflecting cardiac structure and function: it showed a significant positive

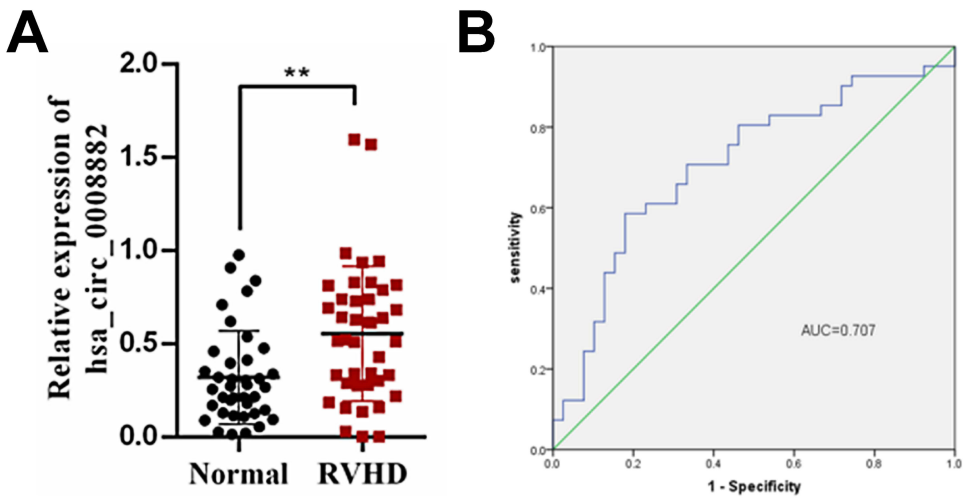

Figure 4 Expression level of hsa_circ_0008882 in RVHD plasma and its diagnostic value. (**A**) The expression level of hsa_circ_0008882 in the RVHD group (n=41) was significantly higher than in the control group (n=39). (**B**) ROC curve and AUC evaluated the potential diagnostic value of hsa_circ_0008882 in RVHD. **p < 0.01.

correlation with left atrial diameter (LAD) (ρ = 0.431, $p < 0.001$) and also with pulmonary artery systolic pressure (PASP) (ρ = 0.331, $p = 0.007$). However, its correlation with left ventricular end-diastolic diameter (LVEDD) did not reach statistical significance (ρ = 0.225, $p = 0.064$). These findings suggest that elevated hsa_circ_0008882 expression not only correlates with the presence of RVHD but may also predict more complex valvular disease (multivalvular heart disease) and more severe cardiac structural remodeling (left atrial enlargement) and hemodynamic abnormalities (pulmonary hypertension).

Clinical Data of the RVHD Group and Control Group

Clinical data of the RVHD and control groups were statistically analyzed with medical history collection, cardiac color ultrasound, and electrocardiogram (Table 3). According to the available data, RVHD patients showed statistically significant differences in LVEDD, LAD, PASP, atrial fibrillation, and multivalvular heart disease on ECG and TTE compared to the control group. The height and weight of the RVHD group were lower than those of the control group, and the proportion of females in the RVHD group was higher.

Relationship Between hsa_circ_0008882 and RVHD

To construct a robust predictive model and avoid overfitting, the LASSO regression model was first employed to screen key predictors from all clinical covariates. At a λ value of 0.0926, LASSO regression identified three variables: gender, history of diabetes, and standardized plasma hsa_circ_0008882 levels (Supplementary Figure 1). These three factors were incorporated into a multivariate logistic regression model for analysis. Results (Table 4) demonstrated that plasma hsa_circ_0008882 levels remained an independent risk factor for RVHD (OR = 3.73, 95% CI: 1.75–7.95, $p < 0.001$) after adjusting for the effects of

Table 2 Correlation Between the Expression of hsa_circ_0008882 and Multivalvular Disease

		r	P
Multivalvular disease	Pearson Correlation	0.286*	0.010*
	Spearman's rho Correlation Coefficient	0.361**	0.001**
LVEDD	Spearman's rho Correlation Coefficient	0.225	0.064
LAD	Spearman's rho Correlation Coefficient	0.431	0.000***
LVEF	Spearman's rho Correlation Coefficient	−0.276	0.022*
PASP	Spearman's rho Correlation Coefficient	0.331	0.007**

Notes: *Correlation is significant at the 0.05 level (2-tailed).**Correlation is significant at the 0.01 level (2-tailed).*$p < 0.05$, **$p < 0.01$, ***$p < 0.001$.

https://doi.org/10.2147/IJGM.S558257

Table 3 Comparison of Clinical Data, ECG, and TTE Results Between RVHD Patients and Control Group

Pathological Factor	Normal Control Group (n=39)	RVHD Group (n=41)	*P*
Age (year)	60 (51, 70)	61 (55, 69)	0.606
Gender (femal/male)	17/22	29/12	0.014*
Height (cm)	163.97±6.65	159.15±7.42	0.003**
Weight (kg)	63.64±10.28	61.35±9.78	0.310
BMI (kg/m^2)	23.63±3.36	24.32±4.19	0.421
Smoking (yes/no)	5/34	3/38	0.476
Drinking (yes/no)	4/35	2/39	0.426
Hypertension (yes/no)	21/18	16/25	0.184
Type 2 diabetes (yes/no)	7/32	2/39	0.084
LVEDD (mm)	45.0 (42.0, 49.0)	49.0 (45.0, 51.0)	0.005*
LAD (mm)	34 (31, 36)	51 (44, 58)	0.000***
IVS (mm)	10.44±1.15	10.79±1.45	0.249
LVEF (%)	65.77±4.69	64.61±6.37	0.359
PASP (mmHg)	30 (28, 32)	42 (32, 48)	0.000***
AF (yes/no)	0/39	16/25	0.000***
Multivalvular disease (yes/no)	0/39	22/19	0.000***

Notes: Continuous variables following a normal distribution were expressed as X ± S and compared between groups using Student's *t*-test. For continuous variables with skewed distributions, data were represented by median (IQR), and the Mann–Whitney *U*-test was used for intergroup comparisons. Categorical variables were expressed as n and analyzed using chi-square tests or Fisher's exact test. *$p < 0.05$, **$p < 0.01$, ***$p < 0.001$.

Abbreviations: BMI, body mass index; LVEDD, left ventricular end-diastolic diameter; LAD, left atrial diameter; IVS, interventricular septum; LVEF, left ventricular ejection fraction; PASP, pulmonary artery systolic blood pressure; AF, atrial fibrillation.

gender and diabetes history. Additionally, being male (relative to female) and having diabetes were identified as protective factors, significantly associated with reduced risk of RVHD.

circRNA Binding miRNA Was Predicted by Sequence Analysis

The potential binding miRNA of circRNA was analyzed using bioinformatics tools and predictive analysis. Using Circbank and circRNA interaction software, five circRNA binding miRNA were obtained, including hsa-miR-3074-5p, hsa-miR-645, hsa-miR-4739, hsa-miR-4710, and hsa-miR-1321 (Figures 5A–E).

Table 4 Logistic Regression with Variable Reduction (Variables Selected by Regularized Regression)

Characteristic	OR	95% CI	p-value
Gender			
Female	—	—	
Male	0.22	0.07, 0.65	0.007
Diabetes			
No	—	—	
Yes	0.06	0.01, 0.48	0.008
circ_0008882_z-score	3.73	1.75, 7.95	<0.001

Abbreviations: CI, Confidence Interval; OR, Odds Ratio.

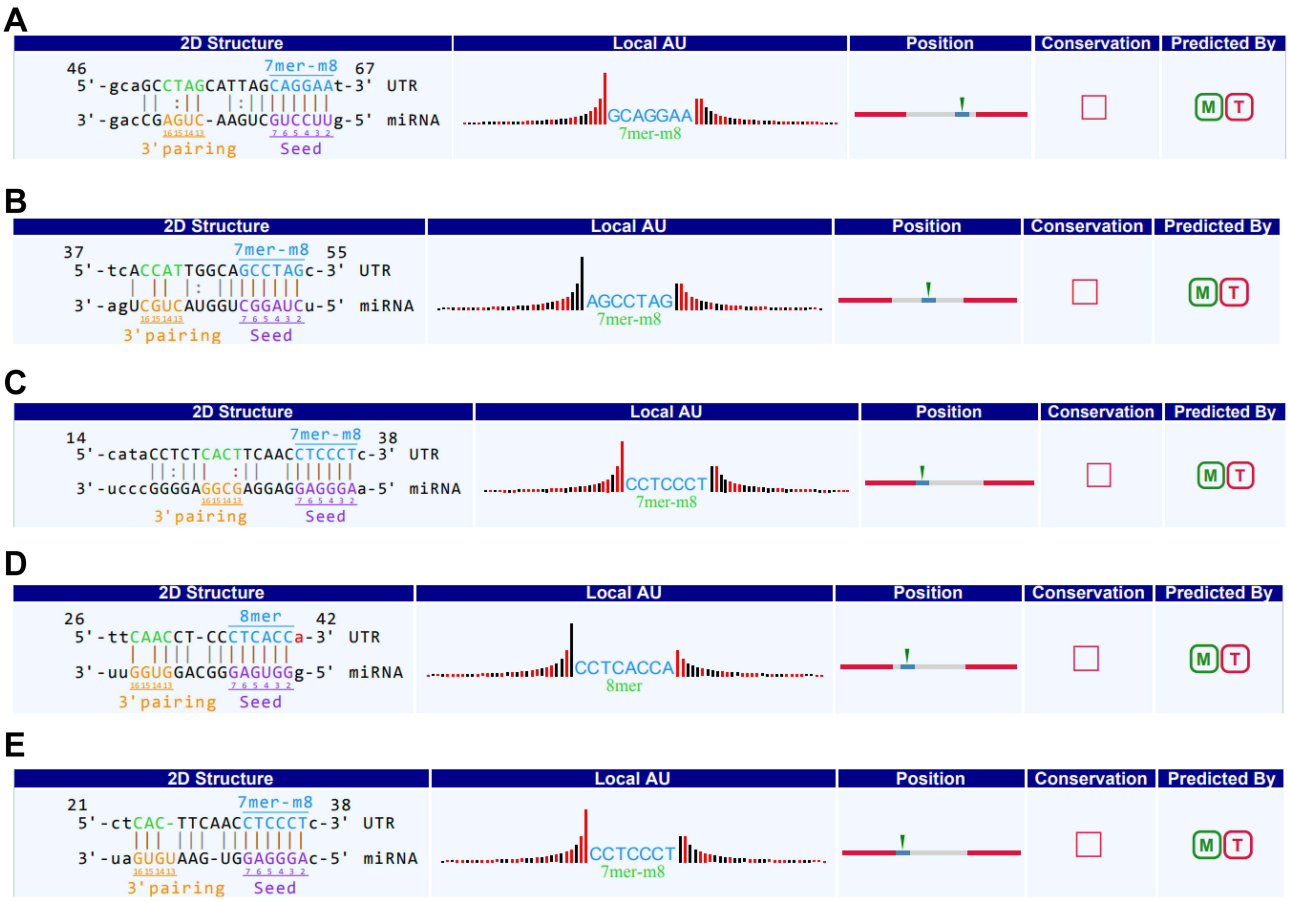

Figure 5 (**A**) Binding site of hsa-miR-3074-5p and hsa_circ_0008882. (**B**) Binding site of hsa-miR-645 and hsa_circ_0008882. (**C**) Binding site of hsa-miR-4739 and hsa_circ_0008882. (**D**) Binding site of hsa-miR-4710 and hsa_circ_0008882. (**E**) Binding site of hsa-miR-1321 and hsa_circ_0008882.

To preliminarily explore the potential functional mechanisms of hsa_circ_0008882, one of its candidate miRNAs, hsa-miR-4739, was selected for validation. Dual luciferase reporter assay results revealed a direct interaction between hsa_circ_0008882 and hsa-miR-4739 (Figure 6), providing preliminary experimental evidence for a potential sponge-miRNA relationship between the two.

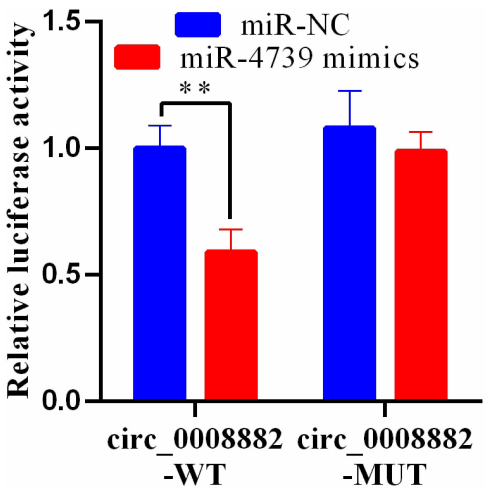

Figure 6 hsa_circ_0008882 and hsa-miR-4739 dual luciferase reporting experiments.

https://doi.org/10.2147/IJGM.S558257

Possible Affected Target Genes

In addition to these miRNAs, bioinformatics tools were used to predict and analyze hsa-miR-584-5p, hsa-miR-4756-5p, hsa-miR-1294, hsa-miR-3146, hsa-miR-155-5p, and hsa-miR-4677-3p, with hsa-miR-4739 being emphasized. Related genes CAMTA2, ZBTB4, NLGN2, CTXN1, NOTCH3, GSK3A, SAMD4B, SCAF1, CDS2, MAP4, DUSP7, DBN1, CD109, HIPK2, MTSS1, NIBAN2, and APLN were found. Through subsequent collection of additional samples (including plasma from 47 RVHD patients and 30 controls, as well as valve tissue from 11 RVHD and 27 non-RVHD cases), the expression levels of CAMTA2 and APLN were re-assessed. The results showed that the expression levels of the protein-coding genes CAMTA2 and APLN were higher in the plasma and valve tissues of RVHD patients than in the control group (Figure 7A–D). Based on bioinformatics predictions and the expression data from this study, it was hypothesized that CAMTA2 and APLN may be potential downstream target genes of the hsa_circ_0008882/miR-4739 axis. However, the direct regulatory relationship between them and the specific function of this regulatory axis in RVHD require further direct confirmation through subsequent studies.

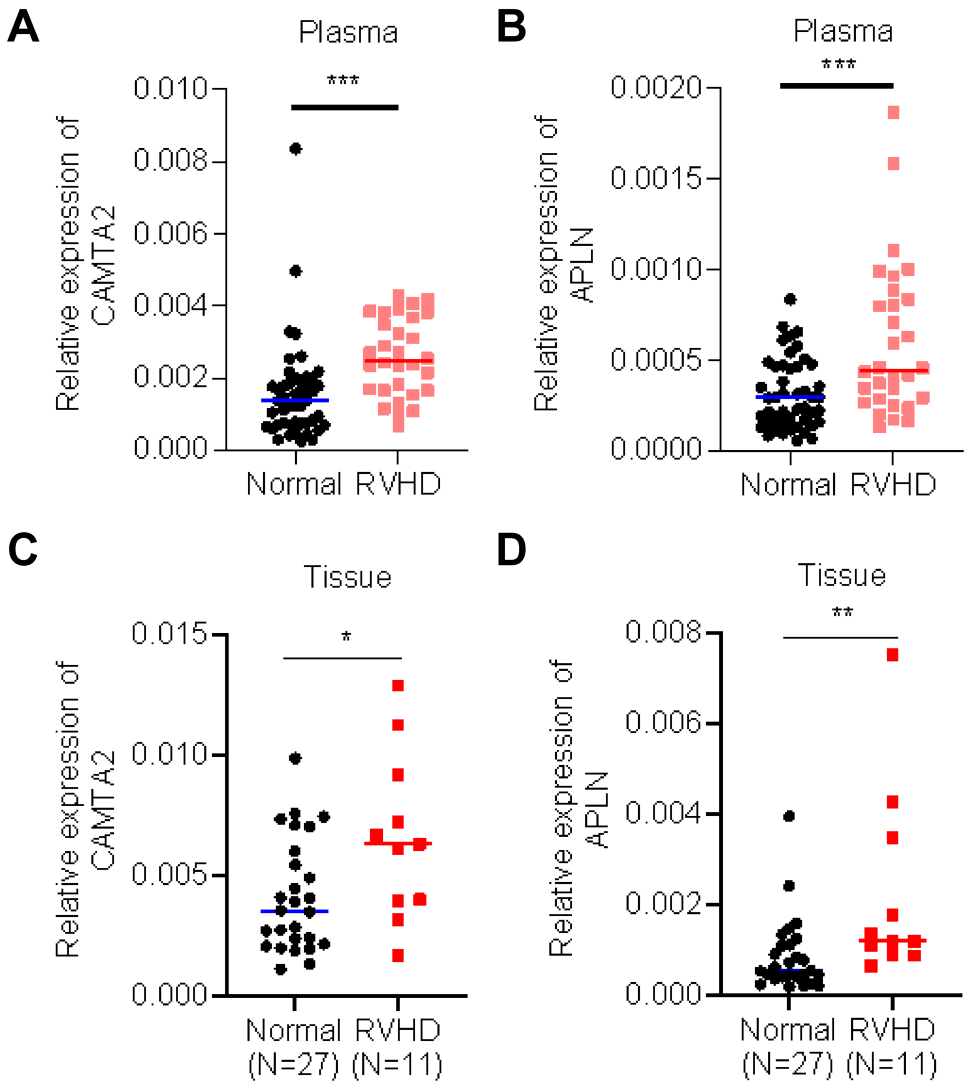

Figure 7 Comparison of relative expression levels of protein-coding genes CAMTA2 and APLN in plasma and tissues between the RVHD group and normal control group. (**A**) The relative expression levels of the protein-coding genes CAMTA2 in plasma differed between the RVHD group and the normal control group, respectively. ***$p < 0.001$. (**B**) The relative expression levels of the protein-coding genes APLN in plasma differed between the RVHD group and the normal control group, respectively. ***$p < 0.001$. (**C**) The relative expression levels of the protein-coding genes CAMTA2 in tissue differed between the RVHD group and the normal control group, respectively.*$p < 0.05$. (**D**) The relative expression levels of the protein-coding genes APLN in tissue differed between the RVHD group and the normal control group, respectively. **$p < 0.01$.

Discussion

CircRNA often functions by binding to miRNA response elements, which captures miRNA and indirectly boosts the transcription levels of their target mRNA. circRNA-miRNA-mRNA network associated with cardiovascular disease has been widely reported.[17–19] In recent years, multiple authoritative reviews have systematically summarized the pivotal roles of circRNAs in cardiovascular diseases such as atherosclerosis, myocardial infarction, heart failure, and aortic aneurysms. Their immense potential as diagnostic biomarkers, prognostic indicators, and therapeutic targets has been widely recognized.[20,21] These studies provide a robust theoretical framework and methodological reference for the field. This research focuses on exploring the clinical application potential of circRNAs in RVHD. We not only validated the expression of hsa_circ_0008882 but also assessed its diagnostic value through multi-model analysis and preliminarily explored its potential mechanisms to provide new candidate biomarkers and molecular mechanism hypotheses for this field.

The relationship between circRNA and cardiovascular disease has been extensively studied. MiR-499 is a heart-specific miRNA that is present in plasma. miR-499 is up-regulated in patients with acute myocardial infarction.[22] This study implies that transcripts specific to the heart could also exist in the bloodstream, with some circulating RNA expression levels potentially correlating with disease states. Thus, assessing transcription levels in the blood is sufficiently reliable for diagnosing heart disease, and circulating circRNAs are promising biomarkers for specific diseases. CircRNA_000203 worsens myocardial hypertrophy by suppressing miR-26b-5p and miR-140-3p, leading to elevated GATA4 levels.[23] There may be a relationship between circRNA hsa_circ_0007990 and an unruptured intracranial aneurysm with an enhanced wall.[24] In coronary heart disease, hsa_circ_0030042 is notably reduced; its overexpression functions as an endogenous eukaryotic initiation factor 4A-III sponge, preventing OX-LDL-induced abnormal autophagy in HUVECs and preserving plaque stability.[25] Hsa_circ_102541 is upregulated in atherosclerosis. Knockdown of circRNA_102541 inhibits cell proliferation and promotes apoptosis of HUVEC cells via miR-296-5p/PLK1.[26] Compared to these studies, this research first revealed the specific upregulation of hsa_circ_0008882 in RVHD. Its diagnostic performance (AUC = 0.707) is comparable to that of circRNAs reported in coronary heart disease,[27] indicating moderate efficacy. This collectively confirms circulating circRNAs as a class of promising biomarkers that still require optimization. hsa_circ_0000437 can affect disease progression in RVHD, indicating the feasibility of circRNA as a potential biomarker.[28]

Regarding its potential for clinical translation, its value must be viewed realistically. Given its moderate discriminatory ability and particularly low sensitivity (0.585), hsa_circ_0008882 is unlikely to serve as an independent diagnostic tool at this stage. However, its high specificity (0.821) suggests it may prove valuable as an adjunct screening indicator. For instance, in primary care or health screening settings, testing plasma hsa_circ_0008882 in suspected patients could reinforce the necessity of referral to tertiary hospitals for definitive TTE diagnosis upon positive results, thereby optimizing healthcare resource allocation. Furthermore, prior literature has documented rare fatal cases of thoracic aortic aneurysm rupture with dissection.[29] Our findings underscore that during the prolonged course of RVHD, novel biomarkers such as hsa_circ_0008882 hold promise for identifying high-risk patients requiring early intervention before irreversible cardiac remodeling and severe complications—such as heart failure—occur.

Notably, this study reinforces the independent association of hsa_circ_0008882 through rigorous statistical modeling. We observed a significant gender imbalance in the RVHD cohort (predominantly female), consistent with the global epidemiological characteristics of this disease.[30–32] By adjusting for gender in multivariate logistic regression, the association between hsa_circ_0008882 and RVHD was independent of this strong confounder, thereby enhancing its robustness as a biomarker. Additionally, we preliminarily observed a trend toward an association between hsa_circ_0008882 and larger LAD length and higher PASP, along with a weaker but significant association with lower LVEF. These findings may relate to RVHD's characteristic involvement of the mitral valve and frequent co-occurrence with atrial fibrillation.[33] Although this requires rigorous validation, it inspires an intriguing future direction: that hsa_circ_0008882 may not only be involved in disease recognition but also correlate with disease severity and hemodynamic burden.

In terms of mechanism, this study provides preliminary clues. Dual luciferase reporter assays confirmed the direct binding between hsa_circ_0008882 and hsa-miR-4739. We hypothesize that hsa_circ_0008882 may sequester hsa-miR-4739, thereby releasing its suppression on downstream target genes such as CAMTA2 and APLN, providing a sponge effect. Combining bioinformatics predictions with synchronous upregulation of CAMTA2 and APLN in RVHD patients,

we hypothesize a potential hsa_circ_0008882/miR-4739/CAMTA2 (or APLN) regulatory axis. It must be emphasized that this remains a hypothesis awaiting validation. The role of APLN in cardiovascular function[34] provides some rationale for its potential involvement in RVHD, but the complete causal chain requires future studies to confirm. This represents a preliminary exploratory finding of our study.

This study has the following limitations. The limited sample size and single-center design may restrict the generalizability of results and raise concerns about overfitting in the initial full-variable model (despite LASSO regression optimization). The insufficient diagnostic performance and inadequate assessment of specificity determine its current "auxiliary" rather than "definitive" role. The absence of certain clinical data (eg, detailed ultrasound classification, medication history) hinder more in-depth analysis of clinical relevance. Most importantly, the mechanism exploration remains at an early stage, constrained by the absence of gain-of-function/loss-of-function experiments in cellular/animal models, validation of miR-4739 levels in patient tissues, and direct evidence of downstream target gene regulation. Although LASSO regression (suitable for high-dimensional data) was employed to optimize model parsimony, the results require external validation in independent datasets given the moderate sample size. Therefore, we recommend the following future directions: validate its diagnostic and prognostic value in larger, multicenter prospective cohorts; incorporate additional cardiac disease control groups to assess specificity; and utilize functional experiments to elucidate its molecular mechanisms in vivo and in vitro.

In summary, this study establishes hsa_circ_0008882 as a relevant, independent potential auxiliary diagnostic biomarker for RVHD. Although its direct application in clinical practice remains distant, it provides a new candidate for the molecular diagnosis of RVHD and opens new avenues for further exploration of the disease pathogenesis.

Data Sharing Statement

Data is available from the corresponding author [GuoFeng Shao] on request.

Ethics Statement

All procedures performed in this study involving human participants were in accordance with the ethical standards of the institutional and/or national research committee and with the 1964 Helsinki Declaration and its later amendments or comparable ethical standards. All subjects were approved by The Affiliated Lihuili Hospital of Ningbo University (IRB No.KY2022PJ222).

Funding

National Natural Science Foundation of China (No.82000365). Ningbo Key Research and Development Program (No.2022Z150). Ningbo Top Medical and Health Research Program (No.2022030107). Ningbo Health Branding Subject Fund (No.PPXK2018-01).

Disclosure

The authors have no conflicts of interest to declare.

References

1. Aluru JS, Barsouk A, Saginala K, Rawla P, Barsouk A. Valvular heart disease epidemiology. *Med Sci*. 2022;10(2).
2. Coffey S, Roberts-Thomson R, Brown A, et al. Global epidemiology of valvular heart disease. *Nat Rev Cardiol*. 2021;18(12):853–864. doi:10.1038/s41569-021-00570-z
3. Roth GA, Mensah GA, Fuster V. The global burden of cardiovascular diseases and risks: a compass for global action. *J Am Coll Cardiol*. 2020;76(25):2980–2981. doi:10.1016/j.jacc.2020.11.021
4. Eleid MF, Nkomo VT, Pislaru SV, Gersh BJ. Valvular heart disease: new concepts in pathophysiology and therapeutic approaches. *Annu Rev Med*. 2023;74:155–170.
5. Peters F, Karthikeyan G, Abrams J, Muhwava L, Zuhlke L. Rheumatic heart disease: current status of diagnosis and therapy. *Cardiovasc Diagn Ther*. 2020;10(2):305–315. doi:10.21037/cdt.2019.10.07
6. Remenyi B, ElGuindy A, Smith SC, Yacoub M, Holmes DR. Valvular aspects of rheumatic heart disease. *Lancet*. 2016;387(10025):1335–1346. doi:10.1016/S0140-6736(16)00547-X
7. Kanani J, Sheikh MI. Ruptured dissecting aorta: an uncommon cause of sudden death—an autopsy study. *Cirugía Cardiovascular*. 2025. doi:10.1016/j.circv.2024.11.009

8. Sanger HL, Klotz G, Riesner D, Gross HJ, Kleinschmidt AK. Viroids are single-stranded covalently closed circular RNA molecules existing as highly base-paired rod-like structures. *Proc Natl Acad Sci U S A*. 1976;73(11):3852–3856. doi:10.1073/pnas.73.11.3852
9. Kristensen LS, Andersen MS, Stagsted LVW, Ebbesen KK, Hansen TB, Kjems J. The biogenesis, biology and characterization of circular RNAs. *Nat Rev Genet*. 2019;20(11):675–691.
10. Li X, Yang L, Chen LL. The biogenesis, functions, and challenges of circular RNAs. *Mol Cell*. 2018;71(3):428–442. doi:10.1016/j.molcel.2018.06.034
11. Jae N, Dimmeler S. Noncoding RNAs in Vascular Diseases. *Circ Res*. 2020;126(9):1127–1145. doi:10.1161/CIRCRESAHA.119.315938
12. Viereck J, Thum T. Circulating noncoding RNAs as biomarkers of cardiovascular disease and injury. *Circ Res*. 2017;120(2):381–399. doi:10.1161/CIRCRESAHA.116.308434
13. Tan WL, Lim BT, Anene-Nzelu CG, et al. A landscape of circular RNA expression in the human heart. *Cardiovasc Res*. 2017;113(3):298–309. doi:10.1093/cvr/cvw250
14. Devaux Y. Transcriptome of blood cells as a reservoir of cardiovascular biomarkers. *Biochim Biophys Acta Mol Cell Res*. 2017;1864(1):209–216. doi:10.1016/j.bbamcr.2016.11.005
15. Shehadeh LA, Hare JM. Ribonucleic acid biomarkers for heart failure is there a correlation between heart and blood transcriptomics? *JACC Heart Fail*. 2013;1(6):477–479. doi:10.1016/j.jchf.2013.10.002
16. Li S, Teng S, Xu J, et al. Microarray is an efficient tool for circRNA profiling. *Brief Bioinform*. 2019;20(4):1420–1433. doi:10.1093/bib/bby006
17. Altesha MA, Ni T, Khan A, Liu K, Zheng X. Circular RNA in cardiovascular disease. *J Cell Physiol*. 2019;234(5):5588–5600. doi:10.1002/jcp.27384
18. Ju J, Song YN, Chen XZ, Wang T, Liu CY, Wang K. circRNA is a potential target for cardiovascular diseases treatment. *Mol Cell Biochem*. 2022;477(2):417–430. doi:10.1007/s11010-021-04286-z
19. Tong KL, Tan KE, Lim YY, Tien XY, Wong PF. CircRNA-miRNA interactions in atherogenesis. *Mol Cell Biochem*. 2022;477(12):2703–2733.
20. Fan Z, Yuan X, Yuan Y. Circular RNAs in coronary heart disease: from molecular mechanism to promising clinical application (Review). *Int J Mol Med*. 2025;55(1). doi:10.3892/ijmm.2024.5452
21. Sygitowicz G, Sitkiewicz D. Involvement of circRNAs in the development of heart failure. *Int J Mol Sci*. 2022;23(22).
22. Adachi T, Nakanishi M, Otsuka Y, et al. Plasma microRNA 499 as a biomarker of acute myocardial infarction. *Clin Chem*. 2010;56(7):1183–1185.
23. Li H, Xu JD, Fang XH, et al. Circular RNA circRNA_000203 aggravates cardiac hypertrophy via suppressing miR-26b-5p and miR-140-3p binding to Gata4. *Cardiovasc Res*. 2020;116(7):1323–1334. doi:10.1093/cvr/cvz215
24. Wu XB, Wu YT, Guo XX, et al. Circular RNA hsa_circ_0007990 as a blood biomarker for unruptured intracranial aneurysm with aneurysm wall enhancement. *Front Immunol*. 2022;13:1061592. doi:10.3389/fimmu.2022.1061592
25. Yu F, Zhang Y, Wang Z, Gong W, Zhang C. Hsa_circ_0030042 regulates abnormal autophagy and protects atherosclerotic plaque stability by targeting eIF4A3. *Theranostics*. 2021;11(11):5404–5417. doi:10.7150/thno.48389
26. Du N, Li M, Yang D. Hsa_circRNA_102541 regulates the development of atherosclerosis by targeting miR-296-5p/PLK1 pathway. *Ir J Med Sci*. 2022;191(3):1153–1159. doi:10.1007/s11845-021-02708-x
27. Sun JY, Shi Y, Cai XY, Liu J. Potential diagnostic and therapeutic value of circular RNAs in cardiovascular diseases. *Cell Signal*. 2020;71:109604.
28. Zhu L, Wang Z, Sun L, et al. Hsa_circ_0000437 upregulates and promotes disease progression in rheumatic valvular heart disease. *J Clin Lab Anal*. 2022;36(2):e24197. doi:10.1002/jcla.24197
29. Kanani J, Modi K. A rare case of sudden death due to rupture of saccular descending thoracic aortic aneurysm with dissection. *Heart Views*. 2024;25(4):270–274. doi:10.4103/heartviews.heartviews_100_24
30. Watkins DA, Beaton AZ, Carapetis JR, et al. Rheumatic heart disease worldwide: JACC scientific expert panel. *J Am Coll Cardiol*. 2018;72(12):1397–1416.
31. Chang AY, Nabbaale J, Okello E, et al. Correction to: outcomes and care quality metrics for women of reproductive age living with rheumatic heart disease in Uganda. *J Am Heart Assoc*. 2020;9(10):e014536. doi:10.1161/JAHA.119.014536
32. Katzenellenbogen JM, Bond-Smith D, Seth RJ, et al. Contemporary incidence and prevalence of rheumatic fever and rheumatic heart disease in Australia using linked data: the case for policy change. *J Am Heart Assoc*. 2020;9(19):e016851. doi:10.1161/JAHA.120.016851
33. Writing Committee M, Otto CM, Nishimura RA, Bonow RO, et al. 2020 ACC/AHA guideline for the management of patients with valvular heart disease: a report of the American college of cardiology/American heart association joint committee on clinical practice guidelines. *J Am Coll Cardiol*. 2021;77(4):e25–e197.
34. Li C, Cheng H, Adhikari BK, et al. The role of apelin-APJ system in diabetes and obesity. *Front Endocrinol*. 2022;13:820002. doi:10.3389/fendo.2022.820002